OS25I-16

Decomposing observations of HF radar derived surface currents by their forcing mechanisms using covariance techniques

Sung Yong Kim†, Eric Terrill, and Bruce Cornuelle

Scripps Institution of Oceanography, La Jolla, CA 92093-0213

syongkim@mpl.ucsd.edu†

1 Abstract

HF radar is an efficient tool for making time series of ocean surface currents, for both scientific and applied purposes. Using observations from an array of 25MHz direction-finding-style systems deployed in the San Diego region, we are developing methods to decompose the surface current data based upon physical processes and frequency bands.

Processes include low frequency pressure gradients, wind forcing, tidal bands centered on K1 and M2, and the residual variance which can not be explained by the previous terms. Early results show that very low frequency (eg. less than 1/15 cpd) surface currents are aligned with sea surface elevation in the same frequency band.([1],[2])

A statistical impulse response function between wind and current was developed which enables the estimation of wind driven currents (and their removal from the dataset). Our approach to addressing the tidally forced component is to examine bands on K1 and M2 as well as their modulation by internal tides.

This dataset also allows us to examine the correlation scales of the surface currents and how they vary in both the cross-shore and alongshore directions. We will present the results of this work, and illustrate how these approaches can be used to develop statistically-based models. Applications of these approaches will be discussed.

2 Observations

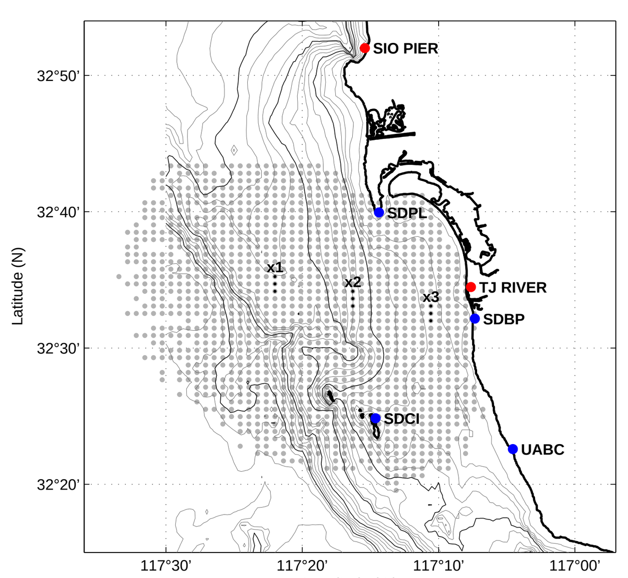

Figure 1: The observation domain of surface currents measured by high-frequency radars at San Diego and the grids for the analysis, which are at least 45% coverage during two years duration The high-frequency radar sites are the SDPL, SDBP, UABC, and SDCI, and wind stations are SIO Pier and Tijuana River.

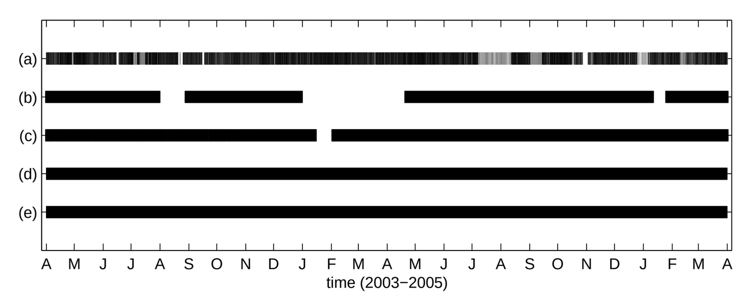

Figure 2: The record history of surface currents, wind and sea level (a) surface currents (b) wind at SIO Pier (c) wind at Tijuana River (d) sea level at San Diego Bay(San Diego) (e) sea level at Outer Harbor(Los Angeles)(The white areas indicate missing data)

3 Analysis

3.1 Basic Statistics

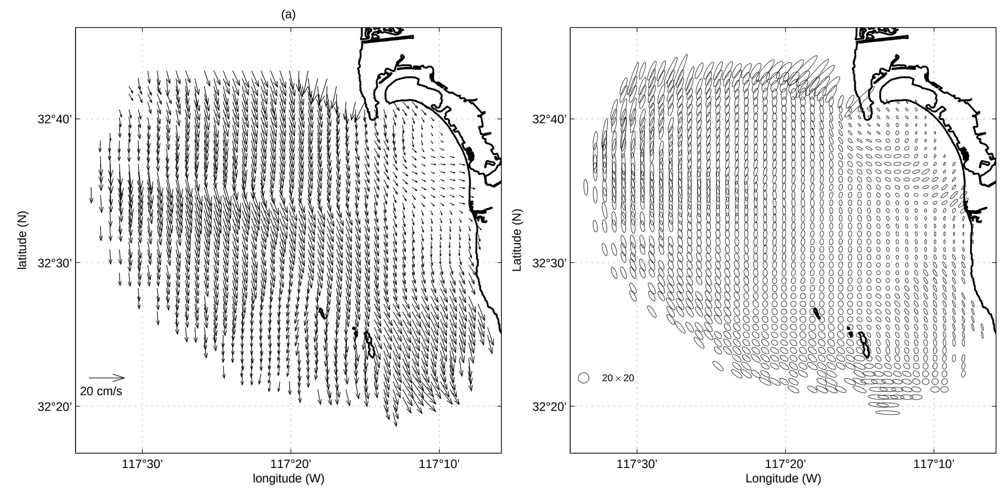

Figure 3: (a) The time mean of hourly surface vector currents shows the dominant south-east-ward currents and complicated current patterns near headland (b) The variance ellipses of surface currents

3.2 Surface current decomposition

The concatenated current vector $\mathbf{u}(\mathbf{x},t) = [u(\mathbf{x},t)\ v(\mathbf{x},t)]^{\mathrm{T}}$ is decomposed into several terms based on driving forces(eg. wind, pressure gradient, and tides).

$$\mathbf{u} = \bar{\mathbf{u}} + \mathbf{u}_w + \mathbf{u}_t + \mathbf{u}_m + \mathbf{u}_r, \tag{1}$$

where $\bar{\mathbf{u}}$, $\mathbf{u}_w$, $\mathbf{u}_t$, $\mathbf{u}_m$, and $\mathbf{u}_r$ denote the mean current, wind-driven current, currents by the tidal constituents, currents by the tidal modulations, which are the low frequency band less than 0.4 (cpd) and bands centered on tide, and rest of it. ($\mathbf{u}_s = \mathbf{u}_t + \mathbf{u}_m$, $\mathbf{u}_t = \mathbf{u}_{K1} + \mathbf{u}_{M2} + \mathbf{u}_{S2}$, $\mathbf{u}_m = \mathbf{u}_{\widehat{L}} + \mathbf{u}_{\widehat{K1}} + \mathbf{u}_{\widehat{M2}}$)

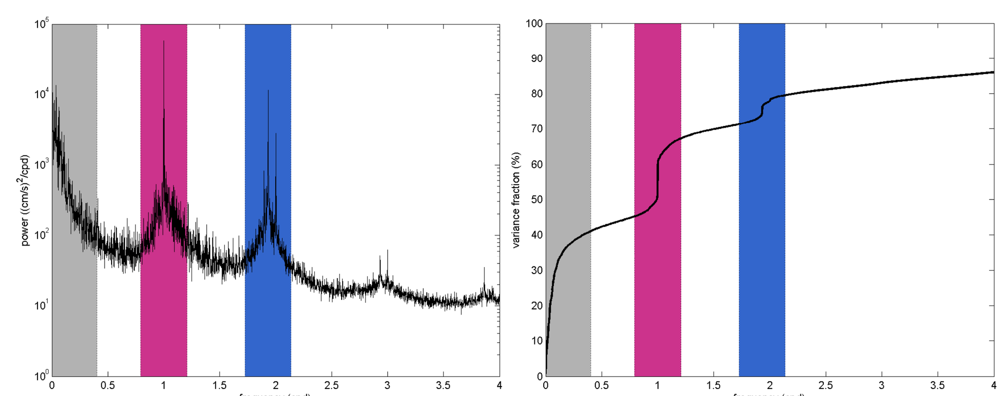

Figure 4: (a) The frequency-bin-averaged power spectrum of hourly surface vector currents at 1337 grids of 45% coverage shows the dominant variances at the low frequency(less than 0.4 cpd), tide(K1 and M2), bands centered on K1(and Coriolis frequency), and M2, their harmonics and residuals. (b) The cumulative variance fraction

3.3 Wind impulse response function

The wind impulse response function of surface currents in finite discrete time domain(Δt), $\mathbf{G}(\mathbf{x}, n\Delta t)$, is defined from the regression by the covariance matrix of wind and current.

$$\mathbf{u}_w(\mathbf{x},t) = \sum_n \mathbf{G}(\mathbf{x}, n\Delta t)\, \tau(t - n\Delta t)\,, \tag{2}$$

where $\tau(t) = [\tau_x(t)\ \tau_y(t)]^{\mathrm{T}}$

The Green's function is the fraction of two covariance matrices. The one covariance matrix is from the wind stress($\tilde{\tau}_p$) stacked with p hours time lag advanced to current and the current driven by all forces($\mathbf{u}_f$). The other one is from the the wind stress($\tilde{\tau}_p$) with time lag itself. The currents uncorrelated with wind are considered as the noise($\mathbf{Q}_1$) in the regression, which is the covariance matrix between the surface current($\mathbf{u}_s$) driven by the spectral forcing and the wind stress($\tilde{\tau}_p$).

$$\mathbf{u}_w(\mathbf{x},t) = \sum_{n=0}^{p} \frac{\langle \mathbf{u}_f(\mathbf{x},t)\,\tilde{\tau}_p^{\mathrm{T}}(t)\rangle}{\langle \tau(t-n\Delta t)\,\tilde{\tau}_p^{\mathrm{T}}(t)\rangle + \mathbf{Q}_1}\, \tau(t - n\Delta t) \tag{3}$$

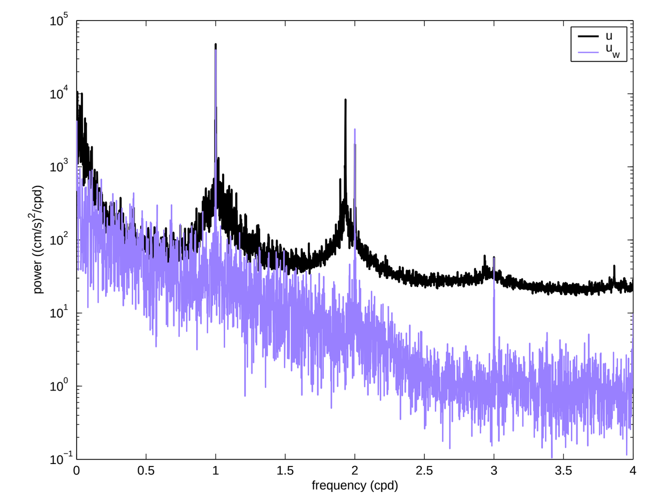

Figure 5: The frequency-bin-averaged power spectrum of currents with all driving forces ($\mathbf{u}$, black line) and wind-driven current($\mathbf{u}_w$, blue line) at all grids

3.4 Spectral forcing

The currents driven by the spectral forcing are classified by the least squares fit with Fourier coefficients($\mathbf{m}$) and its orthogonal basis($\mathbf{G}$), which is the appropriate filter for the time series with missing data.

$$\mathbf{u}_s = \mathbf{G}\mathbf{m} \tag{4}$$

$$\mathbf{m} = (\mathbf{G}^{\mathrm{T}}\mathbf{G} + \mathbf{Q}_2)^{-1}\mathbf{G}^{\mathrm{T}}\mathbf{u}_s\,, \tag{5}$$

where $\mathbf{Q}_2$ is the noise to to make $\mathbf{G}^{\mathrm{T}}\mathbf{G}$ positive definite. The frequency resolution($\Delta\omega$) is 0.0014 cpd for two year hourly time series.

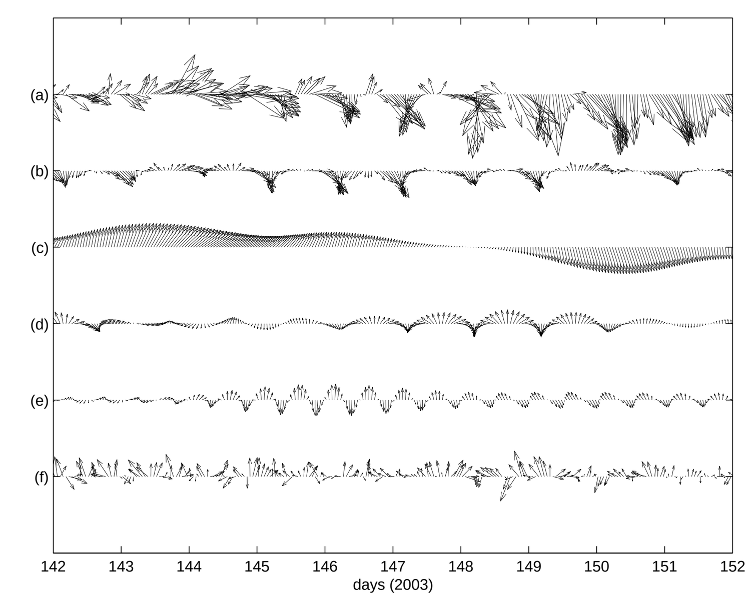

Figure 6: The decomposed time series of surface current at x_1 (a) observed currents, $\mathbf{u}$ (b) wind-driven currents, $\mathbf{u}_w$ (c) currents in low frequency band, $\mathbf{u}_{\widehat{L}}$ (d) currents in frequency band centered on K1, $\mathbf{u}_{\widehat{K1}}$ (e) currents in frequency band centered on M2 , $\mathbf{u}_{\widehat{M2}}$ (f) residual currents, $\mathbf{u}_R$)

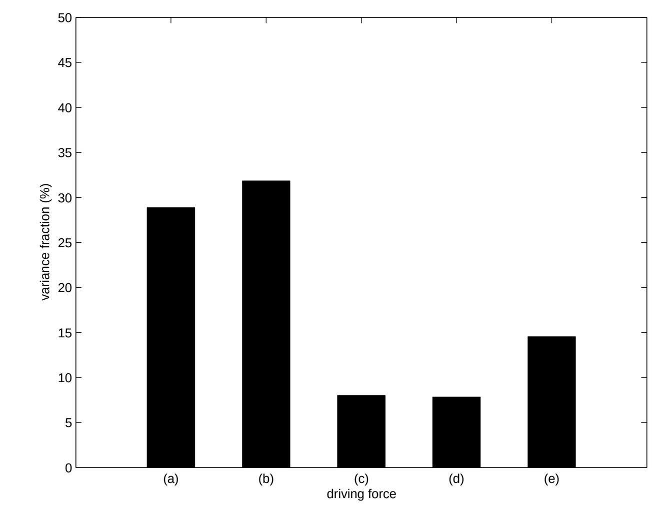

Figure 7: The variance fraction of surface current components (a) wind-driven current, $\mathbf{u}_w$ (b) currents in low frequency band, $\mathbf{u}_{\widehat{L}}$ (c) currents in frequency band centered on K1, $\mathbf{u}_{\widehat{K1}}$ (d) currents in frequency band centered on M2, $\mathbf{u}_{\widehat{M2}}$ (e) residual currents, $\mathbf{u}_R$

3.5 De-correlation scale

The locally averaged correlation coefficients, $\tilde{\rho}(\mathbf{x},\mathbf{x}') \simeq \tilde{\rho}(\Delta x, \Delta y)|_{x=x_0, y=y_0}$, of grids within 4km radius from a reference grid(x_0, y_0) are fitted with exponential function. Since the tails of local averaged correlation coefficients are fluctuating, the grids within $\pm 3\Delta x$ and $\pm 3\Delta y$ are considered.

$$\tilde{\rho}(\Delta x, \Delta y)|_{x=x_0, y=y_0} = \exp\left[-\{a(\Delta x)^2 + b(\Delta x)(\Delta y) + c(\Delta y)^2\}^{\frac{1}{2}}\right], \tag{6}$$

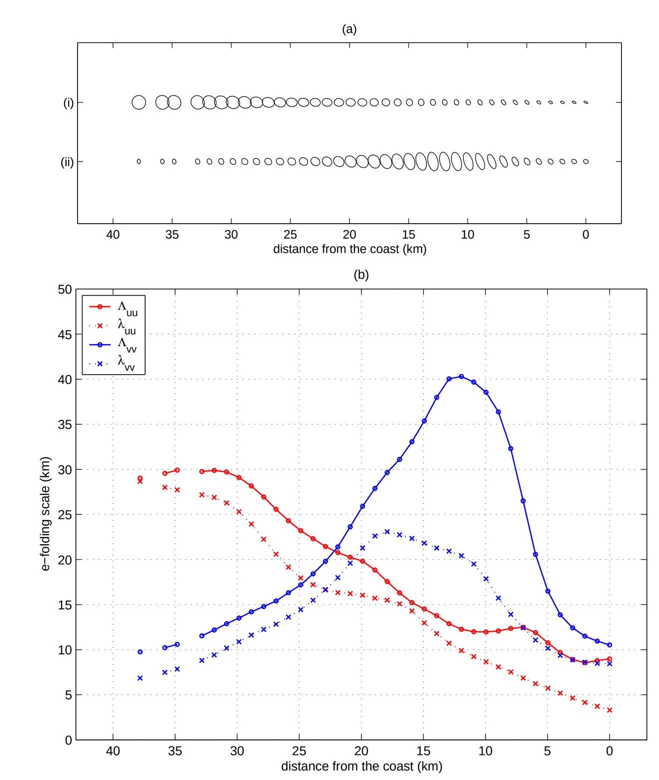

Figure 8: The locally averaged correlation coefficients show the effects of bottom bathymetry on cross-shore currents and those of headlands on the along-shore currents. (a) The ellipses of the correlation coefficients for (i) cross-shore currents and (ii) along-shore currents across the coast. (b) The de-correlation scales across the coast. Λ_{uu} denotes the de-correlation scale of cross-shore currents in cross-shore direction, λ_{uu} is the de-correlation scale of cross-shore currents in along-shore direction. The Λ_{vv} denotes the de-correlation scale of along-shore currents in along-shore direction, λ_{vv} is the de-correlation scale of along-shore currents in cross-shore direction.

3.6 Pressure gradients

The low frequency pressure gradient forcing is estimated from the tidal elevation at the stations along the coastline. We explore the validity of frictional balance between pressure gradient and currents.

$$ru = -g\frac{\partial\eta}{\partial x} \tag{7}$$

$$rv = -g\frac{\partial\eta}{\partial y}\,, \tag{8}$$

where η and r denote the sea surface elevation and friction coefficients($r > 0$, s^{-1})($g = 9.8\ m/s^2$).

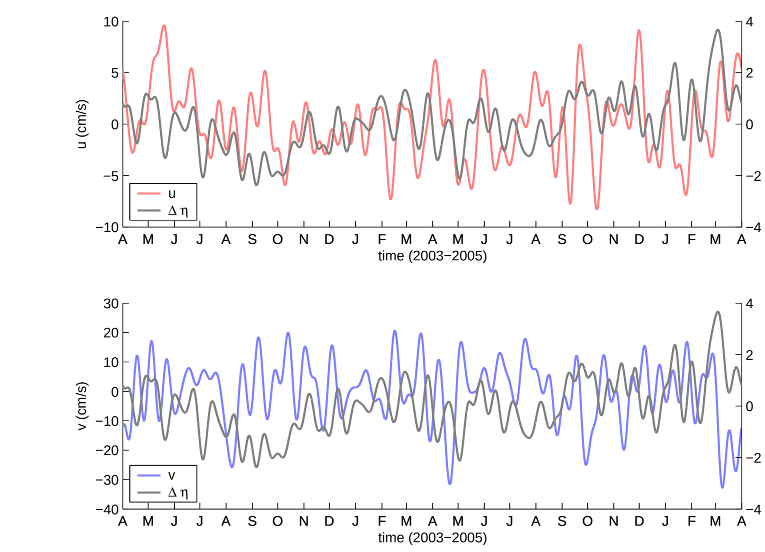

Figure 9: The tidal elevation difference($\Delta\eta = \eta_{LA} - \eta_{SD}$) between Los Angeles(Outer Harbor) and San Diego(San Diego Bay) and surface current at x_1 with very low frequency(T≥ 15 days)

4 Discussion

The decomposition of surface currents in terms of driving forces in the frequency domain assumed that the currents driven by different forces are independent. Therefore, the covariance matrix of each current has its own physical characteristics.

The wind impulse response function is statistically estimated from the observations of wind and currents so that the correlations between the wind-driven currents and non-wind-driven currents are minimized. The wind impulse response function should vary seasonally.

References

[1] H.-H. Essen, K.-W. Gurgel, and F. Schirmer. Tidal and wind-driven parts of surface currents as measured by radar. *Dt. Hydrogr. Z.*, 36(3):81–96, 1983.

[2] W. H. Munk and D. E. Cartwright. Tidal spectroscopy and prediction. *Philos. Trans. Ser. A Math. Phys. Eng. Sci.*, 259(1105):533–581, 1966.

Acknowledgement The wind at Tijuana River is provided by the National Estuarine Research Reserve's (NERR) System-Wide Monitoring Program (SWMP), and sea level elevations are from the Center for Oceanographic Operational Products and Services (CO-OPS) of NOAA.